31st Congress of the International Council of the Aeronautical Sciences

Belo Horizonte, Brazil; September 09-14, 2018

NOVEL JET ENGINE ACOUSTIC LINER WITH IMPROVED BROADBAND NOISE ABSORPTION

K. Hoeschler*, E. Sarradj, N. Modler***, L. Enghardt******
***Brandenburg Technische Universität Cottbus-Senftenberg, **Technische Universität Berlin, *** Technische Universität Dresden, ******German Aerospace Center
all Germany**

Keywords: *Acoustic Liner, Broadband Noise, UHB engines*

Abstract

A feasibility study of a novel type of acoustic liner, suitable for the integration in aero-engines, has been conducted. Back-to-back testing with a standard Helmholtz resonator liner demonstrated that the addition of a flexible material with high intrinsic damping can broaden the effective frequency range and improve the overall noise absorption.

1 General Introduction

Since decades, a substantial share of noise reduction for aero engines is realized through the usage of acoustic liners. These liners are essentially based on the principle of a Helmholtz resonator and consist of a variety of small cells, usually designed as honeycombs with a certain height, a closed back plate and a perforated face sheet, as the boundary to an outer, grazing flow. The actual approach is a combination of the classical Helmholtz resonator principle, a $\lambda/4$ resonator (reactive cancellation) and an additional resistive damping generated by the flow through the holes in the face sheet. The lower the noise absorption frequency, the higher has to be the cell size of the honeycomb. This liner type can be found in aero engines within the intake, the bypass duct and the cold and hot exhaust area. The liners in the cold parts of an engine usually consist of composite materials, like carbon composite for the back plate and face sheet, and aramid fibers for the stiff honeycomb cells; in the hot sections, the cells are made of metal. Such a design has the disadvantage to absorb noise only in a very limited frequency band, if it is used as a single liner (single degree of freedom, SDOF). In aero engine intakes, the selected frequency is usually one of the tonal fan noise frequencies. If two liners of different depths are put on top of each other (double degree of freedom, DDOF, the dividing plate is then also perforated), they can absorb two different, but still narrow frequency bands. A higher number of absorption frequencies close to each other and therefore a more broadband noise reduction is theoretically possible, but would require a corresponding number of liners on top of each other. Due to limited design space, weight and limited efficiency, this design is not applied in aero engines. Therefore, an effective broadband noise reduction with these liner concepts is not achievable. The benefits on the other hand are their robustness and durability, as well as the low weight.

The next generation of aero engines for civil applications will have larger bypass-ratios (BPR >10) in order to improve the propulsion efficiency. These, so called Ultra-High-Bypass - Ratio (UHBR) engines, are characterized by fans with large fan diameters, which will run at a lower rotational speed compared to those currently in use. The lower speed will reduce the tonal fan noise frequency and would require SDOF acoustic liners with an increased cell height to attenuate the tonal noise. However, conventional liners with large cell heights can most likely not be installed due to strict nacelle design constraints on outer diameter in order to minimize the installed engine drag.

In addition, a dedicated low noise design of future engine components will mainly attenuate the tonal contributions of the engine acoustic

emissions. Hence, the noise signature of future aero engines will largely be dominated by broadband noise, which can only be damped efficiently by novel liners.
Europe's ambitious targets for reducing CO_2, NO_x and noise by 2050 are summarized in the *European Flightpath 2050* goals [1]. The consideration of broadband noise reduction will certainly become more and more important in order to achieve the noise targets. The shift in tonal frequencies to lower values in light of the planned future ultra-high-bypass-ratio engines poses an additional challenge. As a consequence of that, new liner concepts will be required in order to accomplish this target.

2 Novel Liner Concept with additional intrinsic material damping

A possible concept to improve the broadband noise absorption is the addition of a further absorbing mechanism to the classical concept as described above. Ideas on how to accomplish this, were published e.g. in [2] and [3]**,** where in the first one a sound damping material is characterized by a pressure sensitive adhesive layer between a honeycomb or corrugated wall and a horizontal face sheet with additional damping performance. The second reference describes a DDOF liner with a high acoustic resistivity material used as the intermediate layer.
The key element of the novel concept described within our paper is additional noise attenuation through the intrinsic damping of a flexible material. The idea was to dissipate acoustic energy by the interaction of the sound field using the flexible walls' viscoelastic deformations. The investigation considered several flexible materials based on a geometrical configuration close to actual acoustic liners.
In order to assess the performance of the various materials, a comprehensive test campaign was undertaken, the results of which were compared with a reference acoustic liner designed to state-of-the-art design rules. Because of time- and cost-restrictions, the traditional internal honeycomb structure of such acoustic liners was substituted by a simplified, easy to manufacture, rectangular shape. For the same reasons, the main structural materials were also replaced as described below.

3 Acoustic Modeling

The novel Helmholtz resonator is supposed to consist of two elementary, acoustically responding components: a conventional Helmholtz resonator (HR) and a damped flexible plate. The aim of the modeling is a preliminary estimate of the resonance frequencies of both individual systems. This allows tuning the geometry and material parameters in order to align these natural frequencies close to each other. As a consequence, the overall transmission loss is expected to become more broadband.
The entire analysis is restricted to the linear plane wave theory, which imposes an upper limit to the analyzed frequency spectrum in a duct, i.e. the first cut-on frequency. Therefore, the desired resonance frequency of the Helmholtz resonator f_H will be chosen far beneath this border. In addition, the HR acts as a $\lambda/4$ resonator [4], which depends mainly on its height l_Z. In order to reduce the participating acoustical phenomena within the model, the first $\lambda/4$ -resonance frequency $f_{\lambda,1}$ is intended to be set far above the corresponding Helmholtz resonance. According to Helmholtz [5], the HR resonance without flow can be well approximated with:

$$f_H = \frac{c_0}{2\pi}\sqrt{\frac{A_L}{V_L(l_H+\pi r_L/2)}}, \qquad (1)$$

where c_0 is the speed of sound, A_L the open area of the perforation, V_Z the volume of the cavity, l_H the height of the perforation hole and r_L its radius. Following [4], the first $\lambda/4$-resonance frequency is determined by:

$$f_{\lambda,1} = \frac{c_0}{4 \cdot l_Z} \qquad (2)$$

Besides, the HR cells also have to fit into the test rig, which is described in detail in section 6. Taking all restrictions into account, f_H is selected to be at approximately 1040 Hz and $f_{\lambda,1}$

at 2860 Hz while the cut-on frequency is located at 2100 Hz. These values yield the following geometric parameters for the HR: l_Z = 30mm mm, V_Z = 10830 mm^3, l_H = 2 mm, r_L = 0.65 mm with a total of nine holes yields to A_L = 12 mm^2.

This is the reference liner which is supposed to be upgraded with at least one damped flexible plate as a substitute for one of its hard sidewalls. Thus, the length and width of the plate is set by the previous HR parameters. The model of the plate is based on the thin plate theory by Kirchhoff-Love, which assumes the plate thickness to be significantly smaller than its width and length. The goal is to determine the thickness and material parameters of the plate such that the plate resonates at frequencies close to f_H, resulting in high deflections and thereby in high energy dissipation via intrinsic material damping, demanding for a material with a high intrinsic loss factor.
According to [6], the plate's resonance frequency (with all edges clamped to the sidewall) of a vibration mode (m, n) can be well approximated with

$$f_{mn} = \left(\frac{t}{2\pi} \sqrt{\frac{E}{12\rho(1-\mu_P^2)}} \right) \cdot \cdot \sqrt{\left(\frac{\mu^2}{L_a^2} + \frac{\nu^2}{L_b^2} \right)^2 + 4\frac{\mu\nu}{L_a^2 L_b^2}(2-\mu-\nu)} \quad (3)$$

where E stands for the Young's Modulus of the plate, ρ for its density, μ_P for its Poisson ratio, L_a and L_b for its length and width, respectively, and t for its thickness. Finally, μ = (m+0.5) π and ν = (n+0.5) π represent the shifted mode orders. However, it must be remarked that this equation only holds for a clamped *in vacuo* plate. Hence, the corresponding resonances will shift when the model is applied to a backed cavity within the novel HR concept. For this purpose, the model is a rough approximation.
As L_a and L_b are predefined by the HR geometry, only the thickness of the plate needs to be tuned for the chosen thermoplastic polyurethane (TPU) composite. This class of rubber-like material is known to achieve high intrinsic loss factors (η = tanδ) [7]. The results show that various TPU types have their first four plate resonance frequencies spread around f_H when the thickness stays beneath 1 mm. Hence, it is made sure that the thicknesses of the TPU samples for the experimental tests fulfill this requirement. The experimental set-up and its results comprising comparisons between the conventional and novel HR concept are presented in section 6.

4 Materials and Manufacturing

4.1 Structure of novel liner concept

As described before, the new acoustic liner concept consists of a perforated face sheet, a rigid back plate and a honeycomb-like prismatic core with a combination of rigid and flexible walls (Fig 1). Several samples with four cavities perpendicular and ten cavities in flow direction were built. The volume V_Z and therefore the dimensions of each cavity (19 mm x 19 mm x 30 mm) were deduced from Eq. (1). All cells perpendicular to the flow direction and every second row of cavities in flow direction were covered with a face sheet having an array of three by three holes of a radius of r_L = 0.65 mm and the height of the perforated hole l_H = 2 mm due to the face sheet's thickness.

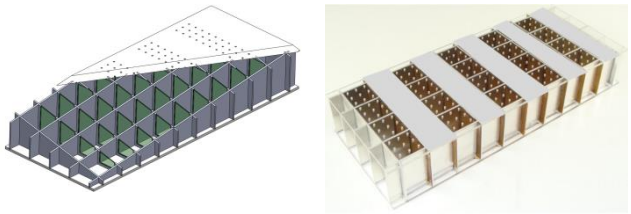

a) b)

Fig 1: Setup of the novel liner concept: a) schematic of acoustic liner with partially flexible walls (green), b) acoustic test sample

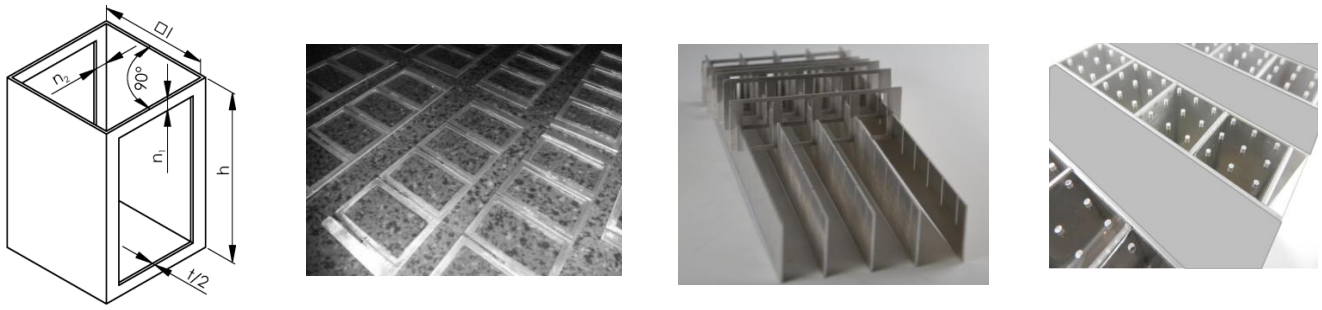

a) b) c) d)

Fig. 2: Fabrication of test samples: a) geometry of the square honeycomb unit cell, b) application of viscoelastic films, c) assembly of rigid and flexible walls, d) bonded face sheet with perforations

The manufacturing of core's walls needs to introduce flexible window-like areas. Thus, an aluminum frame was designed as a supporting structure giving the possibility to attach different films with high intrinsic damping. As materials, one epoxy-based (EP) film and two thermoplastic polyurethane (TPU) films with different thicknesses were applied using suitable adhesive (Table 1). The rigid walls and the frames carrying the flexible areas were made of aluminum ALMG3, H22 with a thickness of 1 mm.

Table 1: Material properties of films based on dynamic mechanical analysis at ambient conditions and a frequency of 100 Hz

Label	EP-0.5	TPU1170A-0.3	TPU1195A-0.1	TPU1195A-0.5
Density in g/cm³	1.2	1.08 [8]	1.15 [8]	1.15 [8]
Young modulus in MPa	6	14	160	160
Tan δ	0.45	0.05	0.20	0.20
Thickness in mm	0.5	0.3	0.1	0.5

The intrinsic damping property of the polymeric material is caused by internal losses during polymeric transitions, e.g. the glass transition. The EP-based material is the result of a material development with the intention to obtain a material with a maximum loss factor at room temperature (as the relevant temperature for the aero-acoustic tests of the prototype) and frequency (1 kHz). This is only possible at the cost of a narrow temperature and frequency range with high damping. Both (commercial available) TPU-materials show a much broader transition range with moderate but significant damping and are possible candidates for operation over a wider temperature range but only for applications where no static load is applied to avoid creeping. There are material classes available with medium damping over a broad temperature range and that are cross-linked, e.g. acrylates, these were not considered within this study.

4.2 Fabrication

There are different technologies to manufacture prismatic honeycombs depending on the materials, the thickness of the materials and the resulting design [9-12]. Wadley describes a strip slotting method for fabrication of triangular and square honeycombs [13]. In this study Wadley's approach is used to build the core with square prismatic cavities. The honeycomb structure was composed of rigid walls and walls with cutouts, that form the edges of the unit cells (Fig. 2). The films were applied upon the walls with cutouts almost stress-free and flat by means of epoxy resin. The edges, the back plate and the face sheet were also bonded by epoxy resin. During the bonding process, the hermetic seal of the joints of the cavities had to be ensured without sealing the perforations in the face sheet. Using this approach, four different samples with flexible walls made of different films (EP-0.5, TPU1170A-0.3, TPU1195A-0.1, TPU1195A-0.5) and one conventional SDOF liner with rigid walls in the same dimensions were fabricated for investigation in this study. In the following, theses liners are called "FlexiS" liners (flexible structure liner).

5 Mechanical Assessment

The feasibility of such a novel liner concept depends not only on the acoustic performance, but also on its mechanical properties, like its compression strength and deformation behavior, to operate it reliably in service. In order to assess the fundamental feasibility with regard to the mechanical behavior of this liner concept, a study was performed in parallel to the acoustic investigations. For this purpose, the geometry was modelled and analyzed by means of the finite element software ANSYS ACP. The geometry of the cutouts, especially the corner radius and upper web height was varied to obtain the sensitivity on the resulting stress distribution. For comparison, a conventional, liner with rectangular shape core and the new liner were analyzed with the same loading. For this study, conventional materials for acoustic liners, such as Meta-Aramid for the walls, carbon fiber and glass fiber-reinforced EP resin for the face sheet and back plate were considered. A representative 3D model was fixed on both sides to simulate a glued and bolted arrangement as in aero engine inlets (Fig. 3). It was conservatively assumed that the flexible films do not stiffen the walls with the cutouts, thus they were neglected.

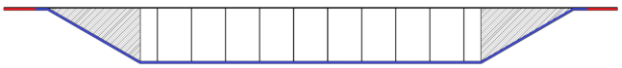

Fig. 3: Fixed boundary condition (red), glued (blue)

The deformation of the honeycomb-like core due to common load cases such as the set of a footstep on the perforated face sheet during maintenance or pressure differences during operating were investigated. The load case with a pressure difference of 10 psi / 0,6895 bar induced the highest stresses.
As expected, the radius at the cutouts is exposed to higher stress levels. The material utilization at the corner of the upper web went up from 12% (without cutout) to about 22%, which is still an acceptable level, see Fig. 4. An increase of the corner radius or web thickness will ovalize the cutout, but can reduce the maximum stress level by 50%. The effect on film vibration and subsequent noise attenuation has not been assessed. The higher flexibility of the walls with cutouts resulted in a 16% higher deflection of the entire structure compared to a conventional liner, which would not affect the outside flow field.

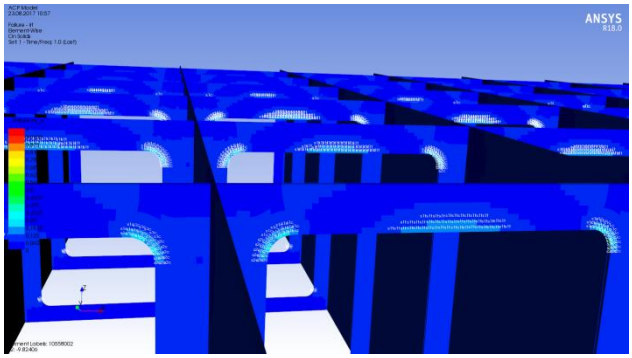

Fig. 4: Material utilization

A further reduction of the maximum stresses in the corners to a lower level was obtained by using a layered composite face sheet with optimized fiber orientation. The utilization of unidirectional layers will shift the loading to the walls perpendicular to the fiber direction and unload the walls parallel to them. In this way lower stress levels at the cutouts can also be achieved.

6 Acoustic test set-up and test results

In order to assess their acoustic performance, the liners were placed in the test section of the DUct aCoustic Test rig - Rectangular cross section (DUCT-R) facility of the German Aerospace Center (DLR) in Berlin. The test rig has a length of about 8 m and consists of two symmetrical sections, each containing several microphones and a loudspeaker for acoustic excitation (see sketch in Fig. 5). The cross section of the rig is 60 mm x 80 mm.
A radial compressor is connected to the upstream part of the duct and provides a grazing flow across the test object with a maximum Mach number of 0.3 at the duct centerline.
Further details of the duct test rig are described by Busse-Gerstengarbe et al. [14]

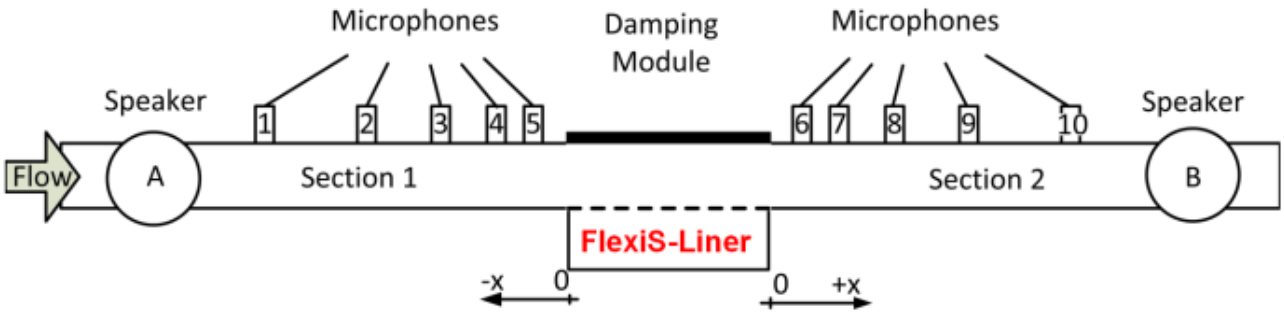

Fig. 5: Sketch of acoustic test rig DUCT-R

The rig has been used extensively during the last years for the investigation of scattering coefficients and impedances of several liner types. It is known to have a very low error in estimated dissipation (1-3%, see e.g. Lahiri [15])

6.1 Experimental Setup

The basic setup for the acoustic measurements is identical to the setup for a conventional SDOF liner. Consecutively, six multi-tones are excited and fed into the rig by either the upstream or the downstream speakers. Thereby, a frequency range from 204 to 2091 Hz with 51 Hz resolution is covered. The overall sound pressure level (SPL) of these multi-tones was adjusted to about 120 dB in maximum, but this could not be fully ensured for all frequencies due to the coupling of the speaker driver and the speaker characteristics. The acoustic investigation was limited to the plane wave regime (cut-on frequency for higher-order modes is about 2150 Hz for the no-flow case).

6.2 Measurement Procedure and Data Processing

For each liner test configuration, two different sound fields are excited consecutively in two separate measurements. Speaker A is used in the first measurement and in the second measurement the same signal is fed into speaker B.

Then, the data of section 1 and section 2 (index 1 and 2) are analyzed separately. Thereby, the sound field is decomposed into upstream- and downstream traveling waves and their respective complex sound pressure amplitudes for each section and measurement. By a combination of all measurements, the influence of end reflections can be canceled out, and the reflection coefficient r and transmission coefficient t for the acoustic pressure can be calculated.

The energetic quantities are obtained applying the acoustic energy flux in a moving medium as given by Blokhintsev [16, 17]. After integrating over the duct cross section A, this yields for the power of the downstream traveling wave P+, respectively the upstream traveling wave P-:

$$P^{\pm} = \frac{A}{2\rho c}(1 \pm M)^2 |\hat{p}^{\pm}|^2, \qquad (4)$$

where M is the mean Mach number of the flow, ρ the density, c the speed of sound, and $\hat{p}^{\pm}$ the complex pressure amplitude of the downstream/upstream traveling wave. Then, the energy coefficients for reflection $R^{\pm}$ and transmission $T^{\pm}$ can be given relative to the pressure coefficients. The dissipation of acoustic energy is expressed by the dissipation coefficient $\Delta^{\pm}$. The dissipation coefficient can be calculated directly from the reflection and transmission coefficients via an energy balance:

$$R^{\pm} + T^{\pm} + \Delta^{\pm} = 1 \qquad (5)$$

The energy of the incident wave is partly reflected, partly transmitted, and partly dissipated inside the damping module. R and T are the power quantities of the reflection and transmission coefficients, while r and t denoted the pressure quantities.

Assuming the same flow conditions and cross sectional area in section 1 and 2, finally, the dissipation coefficients of the test object for the

downstream Δ+ and upstream direction Δ- can be obtained:

$$\Delta^{\pm} = 1 - \left(\frac{(1\mp M)^2}{(1\pm M)^2}|r^{\pm}|^2 + |t^{\pm}|^2\right) \qquad (6)$$

This is an integral value of the acoustic energy that is absorbed while a sound wave is passing the damping module. The dissipation coefficient is used to evaluate the damping performance of the test object, here the FlexiS liner. For most comparisons, the averaged value $\Delta_{avg} = \Delta^{+}/2 + \Delta^{-}/2$ can be used.

6.3 Test Conditions

Four FlexiS liner and in addition a reference liner with fully rigid cell walls have been tested with respect to their acoustic energy dissipation. Certain cells of the prototype liners have been covered with tape in order to enhance the inter-cell wall deflection for the FlexiS liner. By covering the holes in the face sheet of those cells, the direct access of the grazing duct sound field is obstructed. Thereby, a fluctuating pressure difference is present only on one side of the flexible cell walls – allowing for an increased movement of the wall.

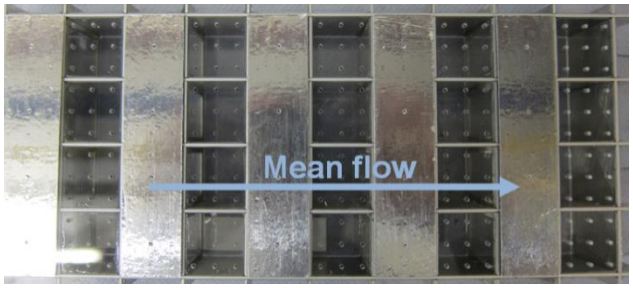

Fig. 6: FlexiS liner top view

In the chosen setup, every second span-wise cell row was covered (see photo in Fig. 6) and only ventilated by a pinhole in order to compensate static pressure differences in the system during operation of the flow duct. Due to their small size, the pinholes should be acoustically insignificant for most of the frequency range of interest in this study.

6.4 Results

Fig. 7 shows the comparison of the averaged dissipation coefficients for the no flow case

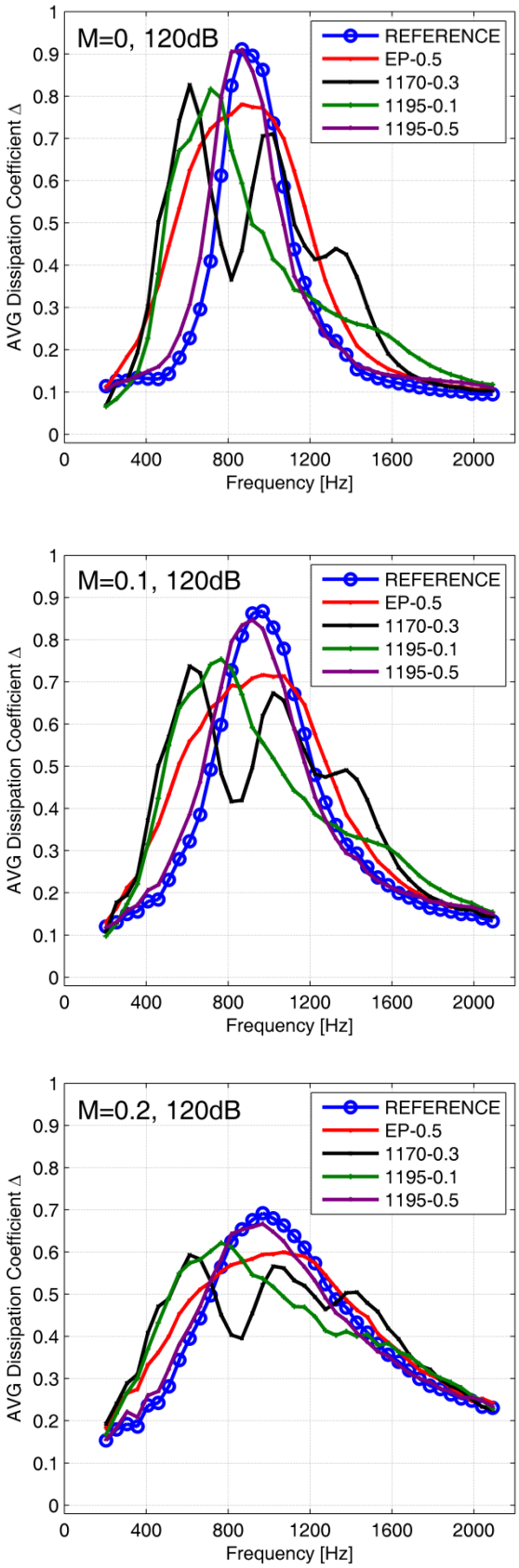

Fig. 7: Average Dissipation for several liners

(M=0) and the cases with moderate grazing flow (M=0.1 and M=0.2). The reference Helmholtz-Resonator liner with rigid walls ("REFERENCE") was prepared the same way (covering every second cell row) in order to compare the same active area for all liner samples.
Most of the FlexiS configurations demonstrate a significant increase of the dissipation in the frequency range from 400 to 800Hz. While the EP-05 material generates a broadening of the dissipation peak, the material 1170-0.3 shows even three local dissipation maxima at 600, 1000 and 1350Hz. The dissipation maximum of the sample with the 1195-0.1 material is shifted from 940 Hz (REFERENCE) to around 750 Hz.
In the case with grazing flow, the observed behavior for the averaged dissipation is comparable to the no flow case as shown in the lower two graphs of Fig. 7 for a grazing flow Mach number of 0.1 and 0.2, respectively. Here, the arithmetic average of dissipation coefficients for up- and downstream direction is displayed. In general, the grazing flow reduces the total dissipation of the liner samples. But since this affects all liner samples including the reference sample with rigid walls, the relative changes in dissipation behavior are similar to the no flow case.
Comparing the dissipation data for 120 dB excitation with the dissipation data for 130 dB (not shown here), there is no significant difference in the observed attenuation behavior. All FlexiS liner samples show a reduction of the maximum dissipation value at the Helmholtz resonance frequency of the rigid cell structure. However, the integrated "overall dissipation" over the entire frequency range is increased (compare Fig. 8 which shows the gain "+" or loss "-" compared to the reference liner).
This verifies the additional damping mechanism by the deflection of the flexible walls with intrinsic material damping.

The actual damping characteristic strongly depends on the chosen material, the specific fixture of the flexible walls, and other acoustic and non-acoustic factors. Further research is needed to better understand the actual physical mechanism, to model the system and to design optimal liners with broadband sound attenuation characteristics.

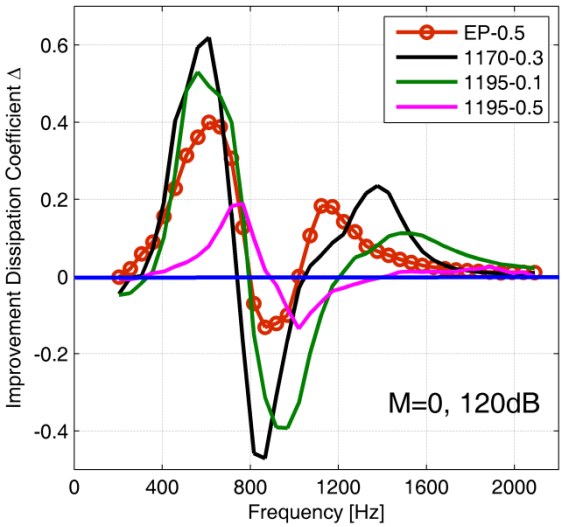

Fig. 8: Improvement (+) or degradation (-) of dissipation coefficient compared to hardwall liner ("REFERENCE")

7 Summary and acknowledgement

A novel type of acoustic liner, suitable for the integration in aero engine inlet und bypass ducts, has been investigated with regard to the possibility of broadening the acoustic damping range and improving the overall noise reduction. Through the addition of films with high intrinsic damping it was possible to add another noise absorption mechanism to the state-of-the-art Helmholtz resonator liner principle. Three different kinds of film material were investigated, an epoxy-based (EP) film and two thermoplastic polyurethane (TPU) films. Samples were designed, built as square prismatic honeycombs with partially flexible walls. This approach obtains a reproducible process for the manufacturing of acoustic liner samples based on the new concept. To ensure a low-cost fabrication concept for large-scale production further fabrication techniques have to be investigated and developed. Each sample was tested in an acoustic wind tunnel. Test conditions, like sound level, frequency and velocity of a grazing flow were varied. The results were compared with a reference standard Helmholtz resonator. It could be demonstrated that an additional overall noise attenuation is

possible and that it will also be possible to shift the resonance frequency to lower values without increasing the dimensions of the liners. The actual damping characteristic strongly depends on the chosen flexible material, the fixture of the films and other acoustic and non-acoustic factors. Subject to the film material, the intrinsic damping characteristic is stable over a certain temperature range.

Further research is needed to better understand the actual physical mechanisms, to model the system and to design optimal liners with broadband sound attenuating characteristics. Further investigations are also required to identify the optimal film material and how to process the material in order to obtain stable damping characteristics in a predefined temperature range over a long operation time.

The feasibility study demonstrated that this novel acoustic liner concept could support the effort to achieve the ambitious noise targets of the *European Flightpath 2050* goals.

Acknowledgment: There were further colleagues involved and made relevant contributions to the results presented in this paper: Dr. Martin Dannemann and Dipl.-Ing. Michael Kucher from the Institute of lightweight design and polymer technology ILK of Technische Universität Dresden, MSc Marcel Mischke from the chair aero-engine design of the Brandenburg Technische Universität Cottbus-Senftenberg, MSc Roman Kisler from the chair Engineering Acoustics of the Technische Universität Berlin and Dr. Karsten Knobloch from the German Aerospace Center (DLR) in Berlin. Colleagues from a further research institute were also part of this research group and contributed significantly to the results: Dr. Olaf Kahle and Dipl.-Phys. Christoph Uhlig, Fraunhofer Institute for Applied Polymer Research IAP.

The research leading to these results has received funding from the German Federal Ministry for Economic Affairs and Energy within the aeronautical research program through the LaKS project under support code 20E1502.

8 References

[1] European Commission. *Flightpath 2050, Europe's Vision for Aviation*. European Commission, 2011.

[2] Fukahori Y. et al.. Sound damping materials. *US Patent 4461796*, 1984.

[3] Bernard et al.. Composite Materials with Acoustic Absorption Properties. *US Patent 3952831*, 1976.

[4] Mechel FP. *Formulas of Acoustics*. 2nd edition, Springer, 2008.

[5] Helmholtz H. Theorie der Luftschwingungen in Röhren mit offenen Enden. *Journal für die reine und angewandte Mathematik*, Vol. 57, No. 4, pp 1-72, 1860.

[6] Leissa AW. *Vibration of Plates*. National Aeronautics and Space Administration, NASA SP-160, United States, 1969.

[7] Drobny JG. *Handbook of Thermoplastic Elastomers*. 2nd edition, Elsevier, 2014.

[8] BASF. *Data sheet. Thermoplastic Polyurethane Elastomers (TPU) Elastollan® – Product Range*, 2017.

[9] Williams CB, Cochran JK and Rosen DW. Additive manufacturing of metallic cellular materials via three-dimensional printing. *Int J Adv Manuf Technol*, Vol. 53, pp. 231–239, 2011.

[10] Del Broccolo S, Laurenzi S and Scarpa F. AUXHEX – A Kirigami inspired zero Poisson's ratio cellular structure. *Compos Struct*, Vol. 176, pp. 433-441, 2017.

[11] Saito K, Pellegrino S and Nojima T. Manufacture of Arbitrary Cross-Section Composite Honeycomb Cores Based on Origami Techniques. *J Mech Des*, Vol. 136, No. 5, pp. 1–9, 2014.

[12] Pflug J, Xinyu F, Lavalaye J, Verpoest I, Bratfisch P and Vandepitte D. *Continuously Produced Honeycomb Sandwich Materials for Automotive Applications*. SAE 2002 World Congress and Exhibition, Detroit, SAE Technical Paper 2002-01-1272, 2002.

[13] Wadley HNG. Multifunctional periodic cellular metals. *Phil. Trans. R. Soc. A*, Vol. 364, pp. 31–68, 2006.

[14] Busse-Gerstengarbe, S., Bake, F., Enghardt, L., and Jones, M. G. Comparative Study of Impedance Eduction Methods, Part 1: DLR Tests and Methodology. *19th AIAA/CEAS Aeroacoustics Conference*, Paper No. 2013-2124, Berlin, Germany, 2013.

[15] Lahiri, C., Sadig, S., Gerendas, M., Enghardt, L., and Bake, F. Establishment of a High Quality Database for the Modeling of Perforated Liners. *Journal of Engineering for Gas Turbines and Power*, Vol. 133, No. 9, pp. 091503-1 – 091503-9, 2011.

[16] Blokhintsev, D. I. Acoustics of a nonhomogeneous moving medium. *NACA, Technical Memorandum 1399*, 1946.

[17] Morfey, C. L. Acoustic energy in non-uniform flows. *Journal of Sound and Vibration*, Vol. 14, No. 2, pp. 159-170, 1971.

9 Contact Author Email Address

mailto: klaus.hoeschler@b-tu.de
mailto: marcel.mischke@b-tu.de
mailto: ennes.sarradj@tu-berlin.de
mailto: roman.kisler@tu-berlin.de
mailto: niels.modler@tu-dresden.de
mailto: martin.dannemann@tu-dresden.de
mailto: eckart.kunze@tu-dresden.de
mailto: michael.kucher@tu-dresden.de
mailto: lars.enghardt@dlr.de
mailto: karsten.knobloch@dlr.de
mailto: olaf.kahle@iap.fraunhofer.de
mailto: christoph.uhlig@iap.fraunhofer.de

Copyright Statement